Density perturbations in a collisional fluid induced by a particle on a slightly-eccentric orbit

Mark Ivan G. Ugalino* and Michael Francis Ian G. Vega II

National Institute of Physics, University of the Philippines Diliman, Quezon City 1101, Philippines
*Corresponding author: mugalino@nip.upd.edu.ph

Abstract

We consider a massive perturber moving along slightly-eccentric orbits through a collisional fluid in flat spacetime. We compute, via a frequency-domain calculation, the density perturbations induced by this massive perturber and reproduce the characteristic spiral wave structure previously computed for circular orbits with time-domain methods. These are needed for extending Barausse's perturbation analysis of relativistic dynamical friction effects on bodies moving through collisional fluids.

Keywords: 95.30.Lz - Hydrodynamics, 95.30.Sf - Relativity and gravitation, 95.10.Eg - Orbit determination and improvement

1 Overview

Dynamical friction (DF), defined as the momentum loss experienced by a massive moving body due to its interaction with its gravitationally induced wake, is very important in theoretical studies of several astronomical systems. The analytic theory of DF for a collisionless system was first formulated by Subrahmanyan Chandrasekhar in his seminal paper [1], the results of which has has been observed in astronomical systems, and applied to numerous numerical simulations over the past several years. Its consequences have been instrumental in theoretically describing the sinking of orbiting galaxies towards their parent galaxy and the dynamical evolution of star clusters near the galactic center, among others. The latter example, however, takes place in a gaseous background, for which the formulation for the process of dynamical friction must be extended. It was not until the finite-time analysis of Ostriker [2] for the straight-line case, and Kim & Kim [3] for circular orbits, that dynamical friction was characterized in both subsonic and supersonic regimes for collisional systems.

A Newtonian treatment, like that of Chandrasekhar's DF formalism, is usually enough to approximate the dynamics of astronomical systems. This is not entirely accurate for cases wherein orbital velocities reach the speed of light, as in extreme-mass ratio inspirals (EMRI), which requires a relativistic extension to accurately describe its evolution. In response, Barausse laid the framework for the relativistic extension of DF in collisional systems by using tools from general relativity [4], while closely following the methods used by Ostriker, and Kim & Kim, that is by analyzing DF effects for straight-line motion and circular orbits in flat spacetime.

It was argued in Barausse's succeeding paper [5] that the gravitational wave emissions of EMRIs may provide a signature of the surrounding gaseous environment (i.e. an accretion disk) by looking at how deviated the observed waveforms are from the predictions of general relativity. However, since the evolution of an EMRI tend to evolve into a very eccentric orbit, an extension of Barausse's work to the slightly eccentric case may be of use in refining our understanding of dynamical friction on the evolution of EMRIs immersed in a tenuous fluid.

This paper serves as a preview to an ongoing project that aims to extend Barausse's relativistic formalism to cases where the perturber travels along a slightly-eccentric orbit through a collisional fluid in flat spacetime. Calculating for the dynamical friction effects requires that we determine the density perturbation function over all space that, in turn, induces the orbit's momentum loss. We present an alternate method adopted from the self-force calculation for slightly-eccentric orbits by Diaz-Rivera et al [6] to solve for the density perturbation function. Throughout the rest of this paper, we used units in which $G = c = 1$.

2 Solving for the density perturbation function

2.1 Source decomposition for slightly-eccentric orbits

It was shown in [4] that in a perturbed flat spacetime background, which has a metric in Poisson gauge [7, 8] given by,

$$d\tilde{s}^2 = -(1+2\phi)\mathrm{d}t^2 + 2\omega_i^{\perp}\mathrm{d}x^i\mathrm{d}t + [\delta_{ij}(1-2\psi) + \chi_{ij}^{\top}]\mathrm{d}x^i\mathrm{d}x^j$$

the evolution of the density perturbation over all space, due to the presence of a moving perturber, is described by the wave equation

$$(\partial_t^2 - c_s^2\nabla^2)\frac{\delta n}{n}(\mathbf{r},t) = 4\pi(T_{tt}+T) \tag{2.1}$$

which, for circular orbits, has an approximate form

$$(\partial_t^2 - c_s^2\nabla^2)\frac{\delta n}{n} = \frac{4\pi M\gamma(1+\mathcal{M}^2c_s^2)}{r^2\sin\theta}\delta(r-R(t))\delta\left(\theta-\frac{\pi}{2}\right)\delta(\phi-\Phi(t)) = 4\pi\rho. \tag{2.2}$$

where $\mathcal{M} = v/c_s$ is the Mach number of the perturber, and c_s is the speed of sound in the fluid. We define the slightly-eccentric geodesic of the perturber by expanding R and Φ about a circular orbit, $R(t) = r_o$, $\Phi(t) = \Omega_o t$, as in [6]:

$$R(t) = r_o + \delta R\cos(\Omega_r t) \tag{2.3}$$

$$\Phi(t) = \Omega_o t + \frac{d\Omega_\phi}{dR}\frac{\delta R}{\Omega_r}\sin(\Omega_r t), \qquad \Omega_\phi \equiv \frac{\mathrm{d}\Phi(t)}{\mathrm{d}t} = \Omega_o + \delta R\frac{d\Omega_\phi}{dR}\cos(\Omega_r t) \tag{2.4}$$

where δR measures the deviation away from circularity, Ω_r and Ω_ϕ are the fundamental frequencies of radial and angular motion, respectively; and, the rate of change of the angular frequency with respect to the radius is given by,

$$\frac{d\Omega_\phi}{dR} = -\frac{2}{r_o}\Omega_\phi$$

Performing a spherical-harmonic decomposition by expanding the delta functions about δR reveals a frequency decomposition of the source with the harmonics of the azimuthal frequency, $\omega_m^o = m\Omega_o$, together with the existence of two other sidebands, $\omega_m^\pm = m\Omega_o \pm \Omega_r$, due to the small eccentricity of the orbit,

$$\begin{aligned}
\rho_{lm}(t,r) &= \oint \rho(t,r,\theta^A)Y_{lm}^*\left(\theta^A\right)\mathrm{d}^2\theta \\
&= \left[\alpha_{lm}\delta(r-r_o)\right]e^{-im\Omega_o t} - \frac{\delta R}{2}\alpha_{lm}\left[\delta'(r-r_o) - m\delta(r-r_o)\frac{2}{r_o}\frac{\Omega_\phi}{\Omega_r}\right]e^{-i(m\Omega_o-\Omega_r)t} \\
&\quad - \frac{\delta R}{2}\alpha_{lm}\left[\delta'(r-r_o) + m\delta(r-r_o)\frac{2}{r_o}\frac{\Omega_\phi}{\Omega_r}\right]e^{-i(m\Omega_o+\Omega_r)t} + \mathcal{O}(\delta R^2) \\
&= \sum_\omega\sum_{l,m}\rho_{lm}^{\omega_m}(r)e^{-i\omega_m t}
\end{aligned} \tag{2.5}$$

where $l = 0, ..., \infty$, $m = -l, ..., l$, $\alpha_{lm} = M\gamma(1+\mathcal{M}^2c_s^2)Y_{lm}^*\left(\frac{\pi}{2},0\right)$ and $\omega = \{\omega_m^o, \omega_m^\pm\}$.

2.2 Solving the wave equation

One can proceed in solving the wave equation by performing a separation of variables in spherical coordinates, which yields

$$\frac{\delta n}{n}(\mathbf{r},t) = \sum_{lm}\Psi_{l,m}(t,r,\theta,\phi) = \sum_{\omega=\omega_o,\omega_\pm}\sum_{l,m}\psi_{lm}^\omega(r)e^{-i\omega_m t}Y_{lm}\left(\theta,\phi\right) \tag{2.6}$$

For convenience, the solution can be divided into the ω_m^o part, ψ_{lm}^o, and the sideband parts, $\delta R\chi_{lm}^\pm$,

$$\frac{\delta n}{n}(\mathbf{r},t) = \sum_{l,m}\left[\psi_{lm}^o(r)e^{-i\omega_m^o t} + \delta R\chi_{lm}^+(r)e^{-i\omega_m^+ t} + \delta R\chi_{lm}^-(r)e^{-i\omega_m^- t}\right]Y_{lm}\left(\theta,\phi\right) \tag{2.7}$$

which, when substituted back to Eq (2.2), gives us a purely radial equation for each l mode with frequency ω_m,

$$\frac{\mathrm{d}^2\psi_{lm}^{\omega_m}}{\mathrm{d}r^2} + \frac{2}{r}\frac{\mathrm{d}\psi_{lm}^{\omega_m}}{\mathrm{d}r} + \left[\left(\frac{\omega_m}{c_s}\right)^2 - \frac{l(l+1)}{r^2}\right]\psi_{lm}^\omega = -\frac{4\pi}{c_s}\rho_{lm}^\omega. \tag{2.8}$$

For each frequency, this wave equation has a solution of the form,

$$\psi^o(r) = \begin{cases} \sum_{l,m\neq 0}A_{lm}j_l\left(\frac{\omega_m^o}{c_s}r\right) + \sum_l A_l r^l + A_{00} & r < r_o \\ \sum_{l,m\neq 0}B_{lm}h_l^{(1)}\left(\frac{\omega_m^o}{c_s}r\right) + \sum_l B_l r^{-(l+1)} - \frac{B_{00}}{r} & r > r_o \end{cases} \tag{2.9}$$

and

$$\chi^{\pm}(r) = \begin{cases} \sum_{l,m} C_{lm} j_l\left(\frac{\omega_m}{c_s} r\right) & r < r_o \\ \sum_{l,m} D_{lm} h_l^{(1)}\left(\frac{\omega_m}{c_s} r\right) & r > r_o \end{cases} \tag{2.10}$$

for the sideband frequencies $\omega_{\pm}$, where j_l and $h_l^{(1)}$ are the spherical Bessel function of the first kind and the spherical Hankel function of the first kind, respectively. The coefficients are obtained by matching the solutions inside and outside the orbital radius $r = r_o$, through imposing continuity and jump conditions for the derivatives at the boundary that were obtained from Eqs (2.5) and (2.8),

$$[\psi^o]_{r_o} = \lim_{\epsilon \to 0^+} [\psi^o(r_o + \epsilon) - \psi^o(r_o - \epsilon)] = 0, \qquad \left[\frac{\mathrm{d}\psi^o}{\mathrm{d}r}\right]_{r_o} = -\frac{4\pi\alpha_{lm}}{c_s^2} \tag{2.11}$$

$$[\chi^{\pm}]_{r_o} = \frac{2\pi\alpha_{lm}}{r_o c_s^2}, \qquad \left[\frac{\mathrm{d}\chi^{\pm}}{\mathrm{d}r}\right]_{r_o} = -\frac{2\pi\alpha_{lm}}{r_o c_s^2}\left(1 \pm m\frac{\Omega_o}{\Omega_r}\right). \tag{2.12}$$

where $[\ ]_{r_o}$ signifies a discontinuous change at the orbital radius r_o.

2.3 Results

A plot of the density perturbation cross-section at the vicinity of the boundary $r = r_o$, at time $t = 0$, as shown in Figure 1a, confirms that we have successfully matched the solutions inside and outside the orbital radius for the main frequency contribution. We can observe in Figure 1b a jump discontinuity between the solutions inside and outside the orbital radius due to the sideband contributions, which confirms that we have successfully implemented the jump conditions that we have imposed earlier.

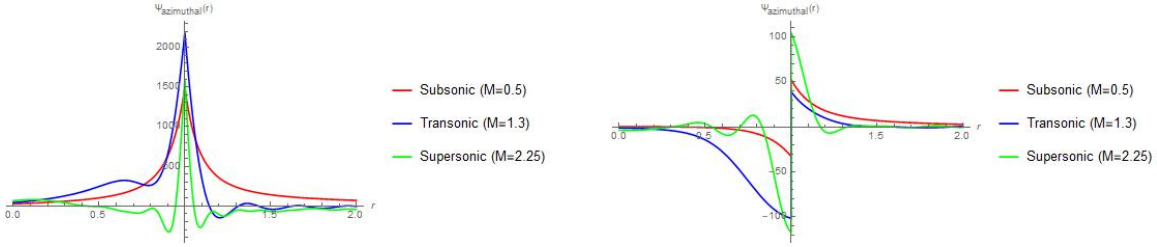

(a) Main frequency (b) Sideband frequencies

Figure 1: Plots of the (a) main frequency contribution, and (b) sideband contributions about the orbital radius, and at $(\theta, \phi) = \left(\frac{\pi}{2}, 0\right)$ for subsonic, transonic and supersonic perturbers.

We can observe the steady state behavior of the density perturbation induced by transonic and supersonic perturbers in a collisional fluid with sound speed $c_s = 0.4$ in Figure 2. Notice that for transonic perturbers, as shown in Figure 2a, there is a long density trail behind the perturber's trajectory for the transonic case, which was already observed in simulations of black hole mergers in gaseous media [9]. In this case, the Mach cone has already engulfed the perturber, which induces larger overdensities within its vicinity. In the supersonic case, as shown in Figure 2c, the Mach cone of the perturber seems to have elongated further, while the density trail that it leaves is wider than in the transonic case. The same physical behavior manifest in the sideband contributions for both transonic and supersonic perturbers, as shown in Figures 2b and 2d respectively. However, the magnitudes of these contributions are subdominant even for a perturbation amplitude δR that is comparable to the orbital radius.

One can infer from these density profiles that the dynamical friction experienced by a perturber in the transonic case is larger than that of the supersonic case, since the overdensity trailing behind the perturber's trajectory in the transonic case is larger. Moreover, we expect that the dynamical friction effects in the radial and azimuthal direction are asymmetric because of the general feature of the overdensity tail that is, it curves towards the circular trajectory of the perturber.

3 Conclusion

We have obtained an expression for the density perturbation induced by a slightly-eccentric orbit on a tenuous fluid through a linear perturbation analysis. Also, we were able to reproduce the density plots produced by Kim and Kim [3] in their Newtonian study of a circular orbit immersed in a collisional fluid. The sideband contributions that was induced by the perturbation that we have introduced are

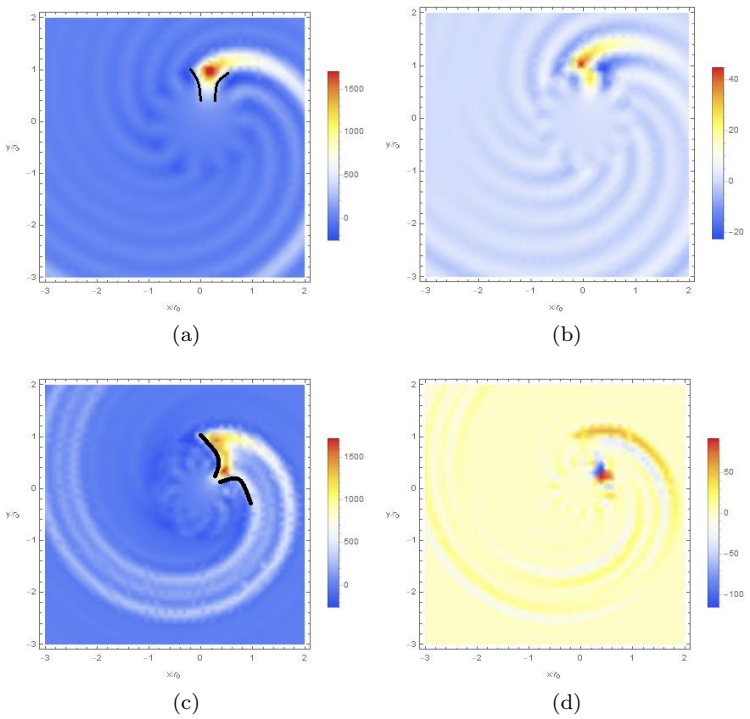

Figure 2: Plots of the steady-state density perturbation induced by a transonic perturber (a,b) with Mach number $\mathcal{M} = 1.3$, and by a supersonic perturber (c,d) with Mach number $\mathcal{M} = 2.25$, moving through a fluid of sound speed $c_s = 0.4$, along a slightly eccentric orbit with $\delta R = 1$. The solid black curves denote the general features of the Mach cone induced by the perturber on the fluid.

subdominant compared to that of the effects that were already present in a circular orbit case. From the derived expressions for density perturbations we can compute the corresponding metric perturbations in our flat spacetime background. These, in turn, will give us the four-acceleration experienced by the perturber, which corresponds to the mechanism of dynamical friction. We leave this calculation for future work.

Acknowledgments

This work acknowledges the support of the University of the Philippines OVPAA through Grant No. OVPAA-BPhD-2016-13.

References

[1] S. Chandrasekhar, I. General Considerations: The Coefficient of Dynamical Friction, *Astrophys J* **97**, 255 (1943).

[2] E. Ostriker, Dynamical Friction in a Gaseous Medium, *Astrophys J* **513**, 252 (1999).

[3] H. Kim and W.-T. Kim, Dynamical friction of a circular-orbit perturber in a gaseous medium, *Astrophys J* **665**, 432 (2007).

[4] E. Barausse, Relativistic dynamical friction in a collisional fluid, *Mon Not R Astron Soc* **382**, 826 (2007).

[5] E. Barausse and L. Rezzolla, Influence of the hydrodynamic drag from an accretion torus on extreme mass-ratio inspirals, *Phys Rev D* **77**, 1 (2008).

[6] L. Diaz-Rivera, E. Messaritaki, B. Whiting, and S. Detweiler, Scalar field self-force effects on orbits about a Schwarzschild black hole, *Phys Rev D* **70**, 14 (2004).

[7] H. Kodama and M. Sasaki, Cosmological perturbation theory, *Prog Theor Phys S* **78**, 1 (1984).

[8] C. Ma and E. Bertschinger, Cosmological perturbation theory in the synchronous and conformal Newtonian gauges, *Astrophys J* **455**, 7 (1995).

[9] A. Escala, R. Larson, P. Coppi, and D. Mardones, The role of gas in the merging of massive black holes in galactic nuclei. I. Black hole merging in a spherical gas cloud, *Astrophys J* **607**, 765 (2004).